

# High-Sensitivity Isothermal and Scanning Microcalorimetry in PNIPA Hydrogels around the Volume Phase Transition

Krisztina László,<sup>\*,†</sup> Katalin Kosik,<sup>†</sup> and Erik Geissler<sup>‡</sup>

Department of Physical Chemistry, Budapest University of Technology and Economics, Laboratory of Soft Matters, Hungarian Academy of Sciences, Budapest 1521, Hungary, and Laboratoire de Spectrométrie Physique CNRS UMR5588, Université J. Fourier de Grenoble, B.P. 87, 38402 St. Martin d'Hères Cedex, France

Received August 9, 2004; Revised Manuscript Received October 7, 2004

**ABSTRACT:** Mechanical and dynamic light scattering measurements show that at 20 °C poly(*N*-isopropylacrylamide) (PNIPA) hydrogels are in good solvent conditions. At this temperature, the average value of the collective diffusion coefficient is  $D = 4 \times 10^{-7} \text{ cm}^2/\text{s}$ . The value of the enthalpy found by isothermal microcalorimetry is roughly twice that reported in the literature. Even at extremely low scanning rates (0.02 °C/min), full thermal equilibrium was not achieved in DSC. Small-angle X-ray scattering measurements confirmed that the gel collapse involves two stages. The first is prompt microphase separation in which the polymer chains form clusters of size approximately 10 nm, separated by distances of several hundred nanometers. The second stage involves slow relaxation and expulsion of solvent, with an estimated diffusion coefficient at 40 °C equal to about  $10^{-17} \text{ cm}^2/\text{s}$ . The slow relaxation of the frozen network is responsible for the hysteresis in the DSC measurements and can explain the discrepancies in the reported values of the enthalpy.

## Introduction

Intelligent soft materials have recently emerged as a topic of intense research activity as their potential is recognized for replacing or acting as substrates for biological tissues or as sensors of biomedical or environmental signals. The operating principle of such devices relies on materials whose volume changes abruptly, i.e., that display a volume phase transition (VPT), when an appropriate stimulus is applied. Poly(*N*-isopropylacrylamide) (PNIPA) is a material that is widely used for this purpose since its VPT in pure water is at a temperature convenient for many applications, close to 34 °C.<sup>1–3</sup> Despite the abundant literature on PNIPA, however, the mechanism of the transition and the thermodynamic parameters governing the phenomenon are incompletely understood, particularly in the collapsed region immediately above the VPT. A knowledge of the material properties in the vicinity of the VPT is essential for any application working in this temperature range.

For many applications the critical operating parameter is the rate of change of volume, i.e., the rate of expulsion of the solvent, both below and above the VPT. This rate is defined on one hand by the size of the specimen and on the other by the collective (mutual) diffusion coefficient  $D$  of the swollen network.  $D$  is different from and always slower than the self-diffusion coefficient of the solvent, observed by nuclear magnetic resonance techniques,<sup>4,5</sup> and can be measured either by dynamic light scattering<sup>6,7</sup> or by direct observation of the change in size of the sample. Above the VPT, however, light scattering measurements are hampered by the strong opalescence of the sample, while direct observations of macroscopically sized specimens are made difficult by the extreme slowness of the relaxation.

In this article, we investigate the transition in PNIPA by combining macroscopic measurements, involving mass balance and high sensitivity isothermal and scanning microcalorimetry, with microscopic observations using light and small-angle X-ray scattering techniques.

## Experimental Section

**Gel Preparation.** 25 mL precursor solutions were prepared by mixing 18.75 mL of a 1 M aqueous solution of *N*-isopropylacrylamide (NIPA) (Wako Pure Chemicals) and varying amounts of a 0.1 M solution of *N,N'*-methylenebis(acrylamide) (BA) (Aldrich) together with 0.25  $\mu\text{L}$  of *N,N,N',N'*-tetramethylethylenediamine (TEMED) (Aldrich) and the appropriate complement of water. Finally, ammonium persulfate (APS) (Aldrich) was added to the mixture, and polymerization was allowed to take place at 20 °C. The cross-link ratios of the gels used in this paper refer to the molar ratio [NIPA]/[BA], which was chosen in the range 75–200. Gel films of thickness 2 mm were cast, while for the modulus measurements samples were made in 1  $\times$  1 cm isometric cylindrical molds. The samples were then dialyzed in water to remove unreacted chemicals. The films were cut into disks of diameter 7 mm, then air-dried, and stored above concentrated sulfuric acid. Cylinders were dried and kept in the same way. Disks used for the microcalorimetry measurements were cut with a maximum diameter of 5.8 mm to avoid geometrical limitation of the swelling in the measuring cell. Powdered specimens were prepared by grinding the film in an agate mortar.

For the swelling measurements the dry disks were equilibrated with Millipore water at 20.0 °C for 7 days. The swelling ratio was determined gravimetrically. The density of the dry polymer,  $d_{\text{PNIPA}}$ , was determined by measuring the density of aqueous solutions of PNIPA at 20.00 °C, using a DMA 58 density meter (Anton Paar, Graz, Austria). Volume additivity was assumed. The value obtained was  $d_{\text{PNIPA}} = 1.115 \text{ g/cm}^3$ .

Stress–strain measurements were performed under uniaxial compression as described by Horkay and Zrínyi.<sup>8</sup> The dry cylindrical samples of different cross-link ratio were equilibrated in water for 7 days at 20.0 °C prior to the experiments.

**Microcalorimetry.** Isothermal and scanning microcalorimetric measurements were made on a MicroDSCIII apparatus (SETARAM). About 5 mg of dry gel samples was placed in contact with 180  $\mu\text{L}$  of Millipore water after a 2 h incubation

<sup>†</sup> Budapest University of Technology and Economics.

<sup>‡</sup> Université J. Fourier de Grenoble.

\* Corresponding author: fax +36-1 463-3767; e-mail klaszlo@mail.bme.hu.

period in the two compartments of the mixing cell under isothermal conditions. At the end of each experiment a second mixing operation was performed under the same conditions to determine the correction for heat generated by the motion of the mixing rod. The temperature for the isothermal experiments was set and maintained at fixed points between 20 and 40 °C with an accuracy of  $\pm 0.001$  °C.

The following protocol was applied in the DSC measurements. About 10 mg of dry gel sample was placed in contact with 500  $\mu$ L of Millipore water and kept at  $T = 10$  °C for 2 h to obtain a stable baseline. The samples were heated to 50 °C and immediately cooled back to 10 °C with the same scanning rate  $dT/dt$ , which was varied between 0.02 and 0.5 °C/min. For repeated cycles a 1 h delay at 10 °C was observed between the cycles.

**Dynamic Light Scattering.** Light scattering measurements were made with an ALV DLS/SLS 5022F goniometer equipped with fiber-optic coupling and an avalanche photodiode, working with a 22 mW HeNe laser and an ALV 5000E multitaue correlator. The swollen gel disks, approximately 8 mm in diameter and of thickness 2 mm, were placed in 10 mm diameter glass tubes containing the accompanying excess solvent. The temperature of the refractive index matching toluene bath was maintained at 20.0 °C with a precision of better than 0.1 °C. Measurements were also made at 32.7 °C. Each gel was measured at the scattering angles 60°, 90°, 120°, and 150°.

As the dominant scattering comes from large-scale static heterogeneities in these gels, the light scattered by the dynamic concentration fluctuations was strongly heterodyned. The fluctuating contribution to the light scattering intensity  $R_{\theta\text{dyn}}$  and its characteristic decay rate were determined as described in ref 7. As  $R_{\theta\text{dyn}}$  displayed no wave vector dependence for this system, only its angular average,  $R_{\text{dyn}}$ , is reported here.

In normal operation with these samples, the automatic beam attenuator generally admitted 3% of the available light into the scattering cell, i.e., approximately 0.6 mW, of which only a small fraction, certainly less than 10%, is absorbed in the sample. At 20 °C, the resulting heat input caused no significant thermal perturbation in the sample. At 32.7 °C, however, closer to the VPT, the heat from the laser beam strongly perturbed the illuminated region, causing large drifts in the scattered light intensity that make those results less easy to interpret.

**SAXS.** Small-angle X-ray scattering measurements were made at the BM2 beamline of the European Synchrotron Radiation Facility, Grenoble, using an incident wavelength of 0.69 Å (18 keV) with sample-detector distances of 68 cm and 1.62 m. The scattered radiation was detected by a 2-dimensional CCD camera (Princeton), with exposure times of 20 s. After azimuthal averaging of the data, standard corrections were made for dark current and the background signal of pure water. To reduce delays in the heating cycle after the room temperature observations, the samples were removed from the temperature control stage and the system raised to 40 °C, whereupon the specimens were reinserted into the sample holder and the measurements started.

## Results and Discussion

In Figure 1 is displayed the degree of swelling for the PNIPA samples of different cross-link densities in the temperature range 10–40 °C. These mass balance measurements show that introducing more cross-links reduces the swelling capacity of the gels but does not modify the temperature of the VPT. The invariance of the transition temperature with cross-link ratio is corroborated by the DSC curves obtained from these samples at the heating rate  $dT/dt = 0.02$  °C/min, illustrated in Figure 2. Similar invariance of the transition temperature was found in the cooling direction.

Well below the transition temperature the gels are in good solvent conditions. Figure 3 shows the variation

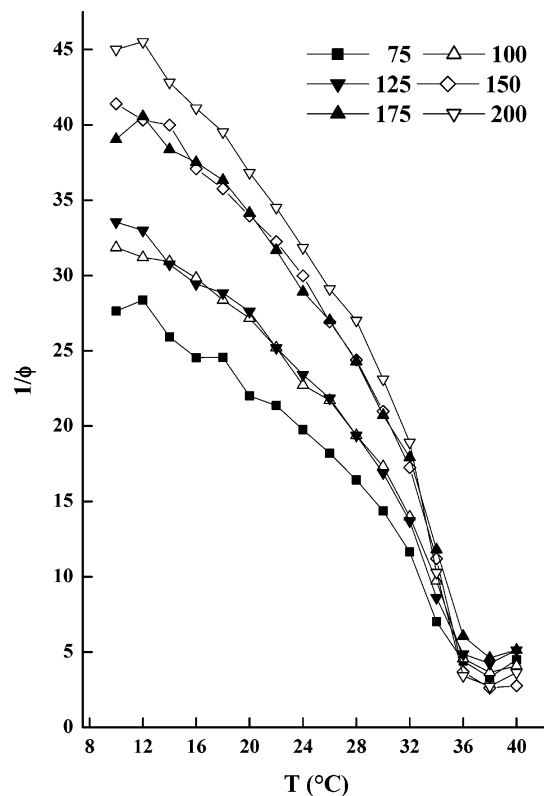


**Figure 1.** Equilibrium swelling ratio  $1/\phi$  of PNIPA gels with different cross-link ratios in water.

of the shear modulus  $G$  at swelling equilibrium at 20 °C as a function of polymer volume fraction  $\phi$ . A least-squares fit yields the power law

$$G = 2.58 \times 10^3 \phi^{2.07 \pm 0.18} \text{ kPa} \quad (1)$$

where the value of the exponent is consistent with that predicted from scaling theory<sup>9</sup> for excluded-volume conditions (9/4).

The collective diffusion coefficient  $D$ , which governs the rate of swelling and deswelling of a gel, and the dynamic component of the scattering intensity, i.e., the Rayleigh ratio  $R_{\text{dyn}}$ , were obtained from dynamic light scattering.<sup>7</sup> Figure 4a shows the resulting values of  $D$  as a function of polymer volume fraction  $\phi$ , both at 20 °C and at 32.7 °C. The error bars are those coming from the averages over the scattering angles. The power law obtained from the weighted least-squares fit through the 20 °C data points is

$$D = 3.1 \times 10^{-6} \phi^{0.57 \pm 0.15} \text{ cm}^2/\text{s} \quad (2)$$

For the measurements at 32.7 °C, however, the scatter in the data is too large to justify using a power law fit.

Figure 4b shows the corresponding variation of  $R_{\text{dyn}}$ , the average of  $R_{\theta\text{dyn}}$  over the four scattering angles. The least-squares fit to the 20 °C data yields

$$R_{\text{dyn}} = 5.9 \times 10^{-5} \phi^{-0.23 \pm 0.17} \text{ cm}^{-1} \quad (3)$$

The exponents in eqs 2 and 3 are both consistent with good solvent behavior (between 0.6 and 0.7 for  $D$  and  $-1/4$  for  $R_{\text{dyn}}$ , respectively). Once again, a power law fit to the 32.7 °C data in Figure 4b is not meaningful (correlation coefficient 0.4), owing to the thermal perturbation from the laser beam described in the Experimental Section.

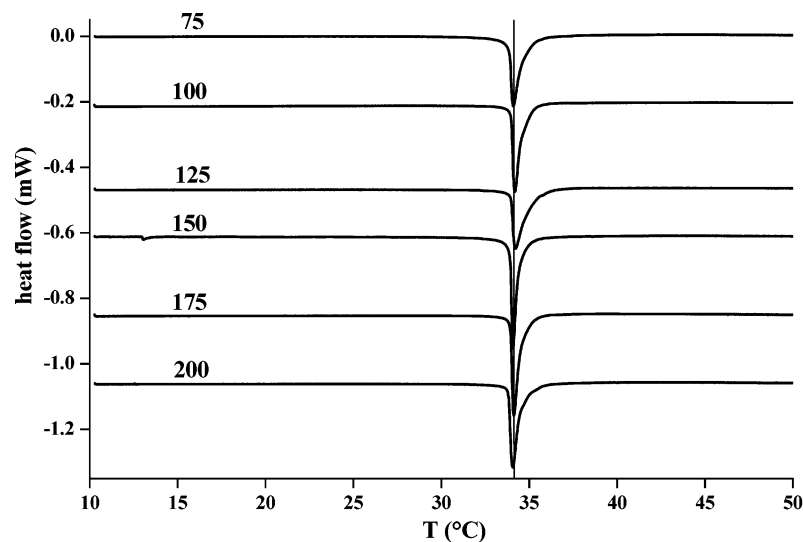


**Figure 2.** DSC heating curves for PNIPA gels with different cross-link ratios in water (ground samples,  $dT/dt = 0.02$  °C/min). The average value of the VPT temperature is  $34.13 \pm 0.06$  °C.

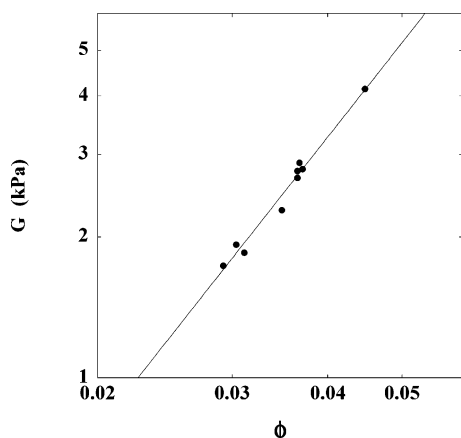


**Figure 3.** Shear elastic modulus  $G$  of PNIPA gels with different cross-link ratios swollen to equilibrium with water at 20 °C. The least-squares power law fit (straight line) yields  $\log G = 3.411 + 2.07 \log \phi$  ( $R^2 = 0.979$ ), where  $G$  is expressed in kPa.

The isothermal swelling enthalpy is illustrated in Figure 5 in the temperature range 20–40 °C. The value of the enthalpy measured at 30 °C ( $-70.7$  J/g) on the powdered PNIPA sample (cross-link ratio 150) is about twice as large as that reported in the literature.<sup>3,10,11</sup> In this figure swelling enthalpies of ground and disk samples of cross-link ratio 150 are compared. No observable difference can be seen between the two sets of data, demonstrating that the resulting system is practically in equilibrium. In the DSC measurement, however, the curves of the same disk samples exhibit bimodal behavior at the scanning rate of 0.02 °C/min, in both the heating and cooling cycles (Figure 6, solid lines). (Similar behavior has already been observed by Kawasaki et al.<sup>3</sup> in heating cycles at higher scanning rates.) In contrast, in the present measurements, the powdered sample exhibits single mode character at  $dT/dt = 0.02$  °C/min. As is to be expected, the size of the specimen is a controlling factor in the VPT. To reduce this effect in the subsequent calorimetric measurements, only powdered samples were investigated.

The shape of the DSC curves is also sensitive to the scanning rate, especially in the cooling cycle. Figure 7 shows the heat flow, normalized by the scanning rate,

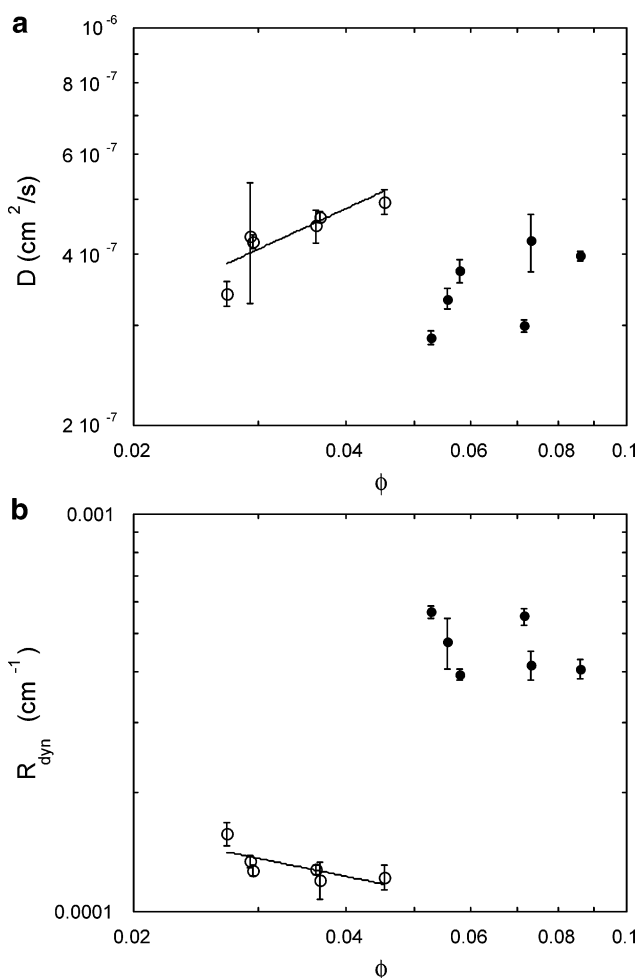


**Figure 4.** (a) Collective diffusion coefficient  $D$  of PNIPA gels of different cross-link ratios as a function of polymer volume fraction  $\phi$  at equilibrium swelling in water at 20 °C (open symbols). At 32.7 °C (filled symbols) the data are too scattered to yield a meaningful power law fit. (b) Rayleigh ratio of dynamically scattered light from PNIPA gels with different cross-link ratios swollen to equilibrium with water at 20 °C (open symbols). The least squares straight line is given by  $\log(R_{\text{dyn}}) = -4.23 - (0.23 \pm 0.17) \log \phi$ . At 32.7 °C (filled symbols) the correlation coefficient ( $R = 0.4$ ) is too low for a power law fit to be meaningful.

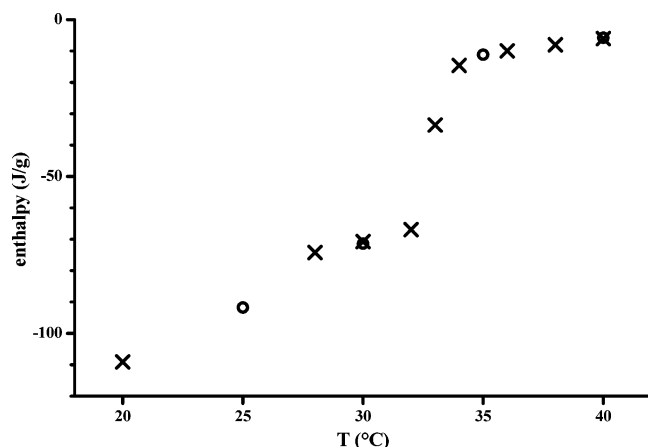


**Figure 5.** Enthalpy of swelling in excess water measured by isothermal microcalorimetry on PNIPA gel (cross-link ratio 150) in disk (O) and powder (x) samples.

as a function of  $dT/dt$ . With increasing scanning rate these exothermal cooling peaks gradually split, revealing the two distinct processes contributing to the VPT. It is particularly striking that the high temperature shoulder in the cooling cycle starts at temperatures *above* the transition. Since it precedes the transition, this phenomenon cannot be attributed to lag in the detection. When the fast cooling is preceded by a slow heating cycle, the shoulder vanishes.

The integrated heat flows obtained from the present experiments yield values (Table 1) that are consistent with our isothermal data, i.e., significantly larger than those reported in the literature, for which the DSC measurements were recorded at higher scanning rates (0.1–10 °C/min).<sup>3,10,12–17</sup> Furthermore, the absolute values of the integrated heat flows obtained at the slowest scanning rate in Figure 8 show that the exothermic cooling peak almost always remains greater than that of endothermic heating. It is difficult to attribute this systematic tendency to the statistical uncertainty of the measurements (5%). It follows that, even for  $dT/dt = 0.02$  °C, the gels are not in full thermodynamic equilibrium during the temperature scan and also that the heating cycle tends to underestimate the integrated heat flow.

To elucidate the mechanisms involved in the VPT, SAXS measurements were undertaken below and above the phase transition on a gel sample with cross-link ratio 150. In the wave vector range explored, the signal from the fully swollen network below the VPT (Figure 9) can be described by an Ornstein–Zernicke expression of the form

$$I(q) = \frac{I(0)}{1 + q^2\xi^2} \quad (4)$$

where  $q$  is the scattering wave vector and the value of the correlation length characterizing the osmotic fluctuations in the gel is found to be  $\xi = 38$  Å (dashed line). When the temperature was raised to 40 °C, a prompt transformation in the shape of the scattering function occurred to a power law with a negative slope  $n \approx 3.7$ . The corresponding surface fractal dimension,<sup>18</sup>  $D_s = 6 - n = 2.3$ , can be interpreted as being due to scattering from large objects with rough surfaces. At the transition, the samples immediately become white, indicating that the size of the scattering units is of the order of the wavelength of light, i.e., several thousand angstroms. The rapidity of the microphase separation requires that the polymer chains remain highly mobile as they aggregate and that the resulting polymer clusters be separated by water-rich regions of this size. This scenario is consistent with the model proposed by Shibayama.<sup>11</sup> Owing to the inhomogeneous frozen-in elastic constraints in this state, the gel is far from thermodynamic equilibrium. When the sample is kept at 40 °C for several hours, the slope of the SAXS curve gradually steepens to its final value  $-4$ , the signature of scattering from smooth surfaces.<sup>19</sup> Figure 10a shows the difference  $\Delta I(q)$  between the signal measured at times  $\tau$  that at the longest delay time. This difference can be fitted approximately to a Debye–Bueche expression of the form

$$\Delta I(q) = \frac{\Delta I(0)}{(1 + q^2a^2)^2} \quad (5)$$

where  $a$  is the radius of the scattering centers. The two curves displayed yield  $a = 90$  Å and 120 Å for  $\tau = 1000$  and 17 000 s, respectively, suggesting a slow increase

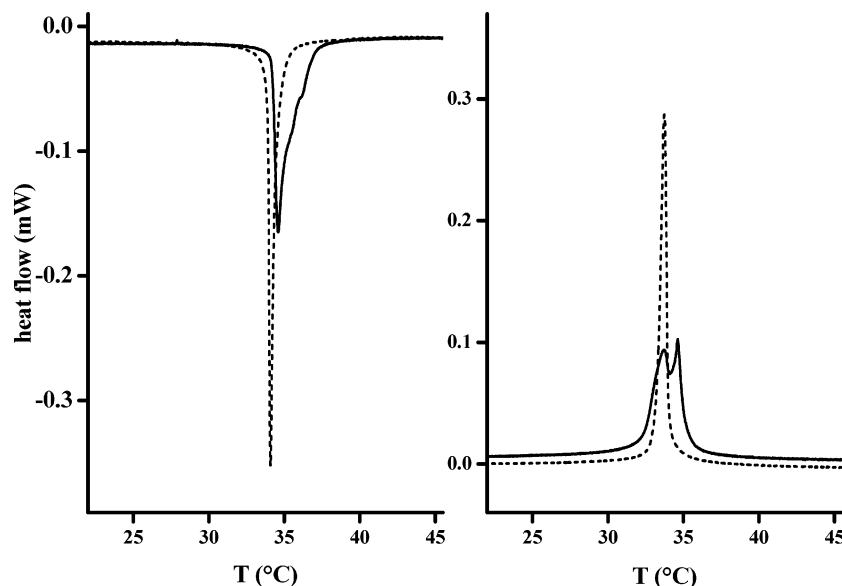


**Figure 6.** DSC of PNIPA gel (cross-link ratio 150) in disk (solid line) and powder (dotted line) samples ( $dT/dt = 0.02$  °C/min) in the vicinity of the VPT temperature in the endothermic heating (left) and exothermic cooling (right) cycles.



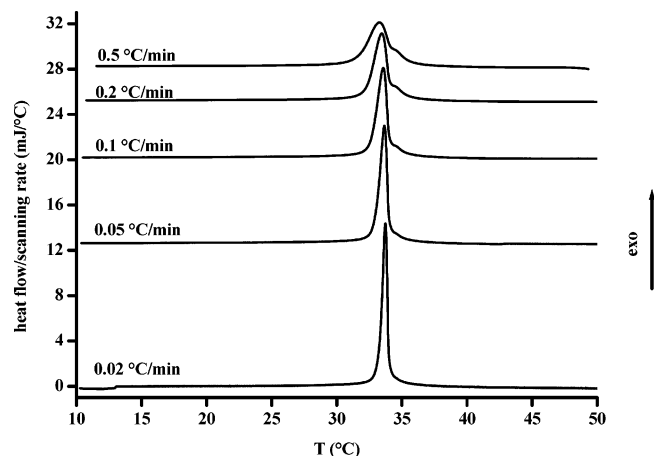


**Figure 7.** DSC measurement of heat flow normalized by the scanning rate for powdered PNIPA gel (cross-link ratio 150) at different cooling rates. With increasing scanning rate the peaks broaden and a distinct shoulder emerges at the high-temperature side. The integrated heat flow changes from  $-62.1$  to  $-65.1$  J/g when the scanning rate is decreased from  $0.5$  to  $0.02$  °C/min.

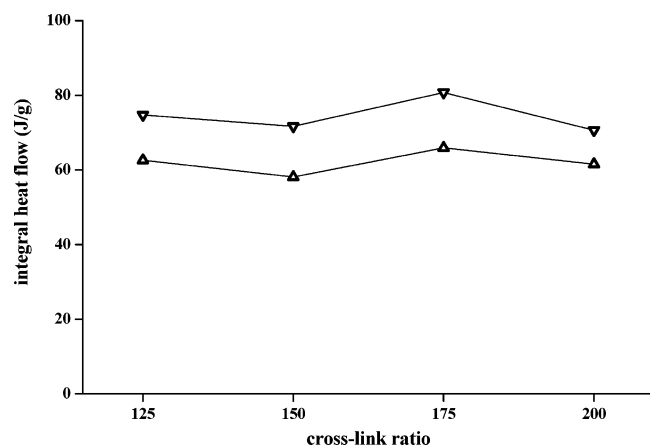


**Figure 8.** Absolute value of the integrated heat flow from DSC measured on PNIPA gels with different cross-link ratios in water in heating ( $\Delta$ , endothermic) and cooling ( $\nabla$ , exothermic) cycles. The difference between the two sets of data indicates hysteresis.

**Table 1. Parameters Derived from the DSC Heating Curves for PNIPA Gels with Different Cross-Link Ratios in Water ( $dT/dt = 0.02$  °C/min, Ground Samples)**

cross-link ratio	heating cycle			cooling cycle		
	onset temp (°C)	peak position (°C)	integral heat flow (J/g)	onset temp (°C)	peak position (°C)	integral heat flow (J/g)
75	33.8	34.1	60	34.0	33.7	-63
100	33.2	34.1	66	34.0	33.6	-62
125	33.9	34.2	63	34.0	33.6	-75
150	33.9	34.1	62	34.0	33.7	-72
175	33.9	34.1	66	33.9	33.6	-81
200	33.8	34.1	62	33.8	33.5	-71

with time of the thickness of the clusters, while the amplitude of the signal decreases. The statistical noise in the difference signal, however, is too large for a reliable decomposition of both the amplitude and the radius. Instead, power law behavior, illustrated in Figure 10b, is assumed over the limited  $q$  range. This approximation allows the time evolution of the apparent slope  $n$  to be determined. Figure 11 shows that the resulting values of  $n$  decay exponentially to  $-4$  with a time constant  $\tau_0 \approx 10^4$  s.

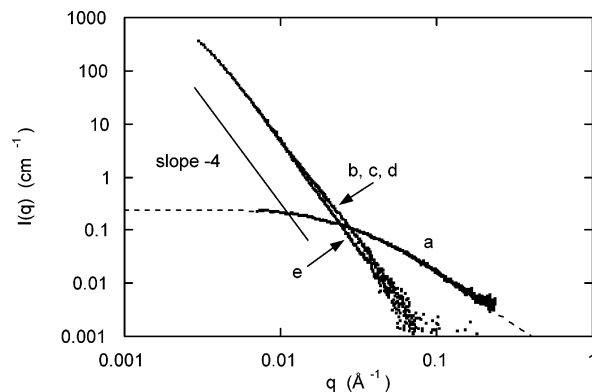


**Figure 9.** SAXS response of PNIPA gel (cross-link ratio 150) at  $25$  °C (a) with curve fitted to eq 4 (dashed line). When the temperature is raised to  $40$  °C, the scattering curve transforms to an approximately power law behavior (b) with a slope of about  $-3.7$ , observed after  $1000$  s. Curves c ( $2000$  s) and d ( $4000$  s) are indistinguishable from curve b. The final curve e ( $30\,000$  s) has a slope of  $-4$ , corresponding to scattering from smooth surfaces.

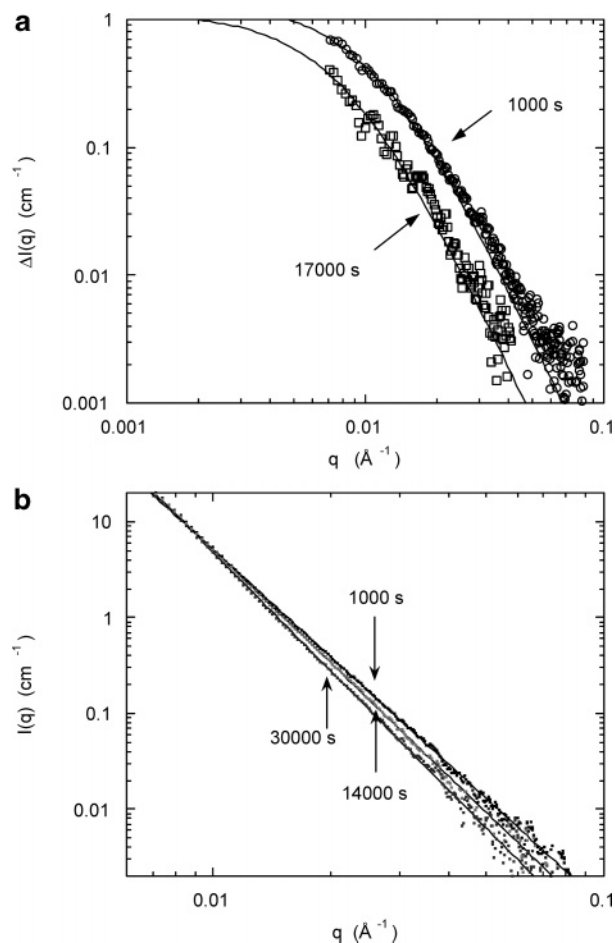


**Figure 10.** (a) Scattering intensity difference at high- $q$  with fits to eq 5 (continuous curves). (b) Detail of SAXS curves at three different times after temperature jump. Only 30% of the data points are plotted in each spectrum. The straight lines are the power law fits.

When combined with the above values of  $a$ , this result implies a diffusion coefficient for the late reorganization of approximately  $a^2/6\tau \approx 10^{-17}$  cm<sup>2</sup>/s. This value is some 10 orders of magnitude smaller than that observed by DLS in the swollen gels (Figure 4a) and is typical of the glassy state. The findings thus indicate that the initial microphase separation is fast because the mobile

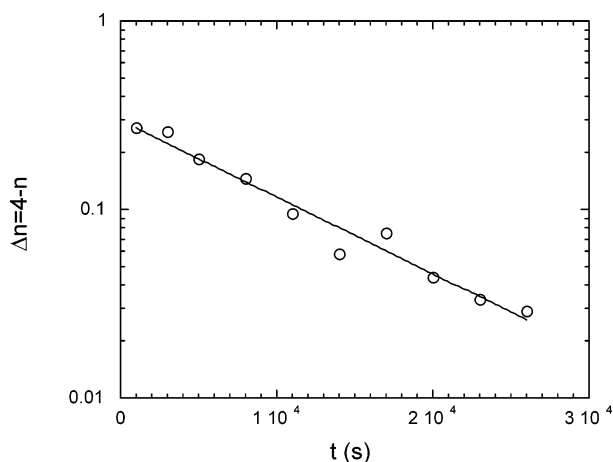


**Figure 11.** Change in power law slope,  $\Delta n = 4 - n$ , of SAXS response as a function of time after temperature jump. The least-squares fit shown is an exponential decay with time constant  $\tau_0 = 1.07 \times 10^4$  s.

polymer chains move relatively freely until they aggregate into glassy clusters, while the extremely slow elastic relaxation of the frozen network is responsible for the hysteresis in the DSC measurements.

Although SAXS assigns numerical values to the cluster size  $a$ , this information alone is not sufficient to determine their geometrical shape in the frozen state. However, the space-filling consideration that the overall volume of large specimens does not change instantaneously at the VPT implies that initially the polymer aggregates are elongated bundles, rather than globular clusters. By contrast, the gradual loss of intensity of the extra scattering and the modest increase observed in the thickness  $a$  at later stages could be consistent with the development of polymer sheets, i.e., a bubblelike structure.

In the cooling cycle, the shoulder on the high-temperature side of the peak, illustrated in Figure 7, corresponds to relaxation of the frozen-in constraints. It may be deduced that in this narrow temperature range the weakening hydrophobic interaction allows a few water molecules to plasticize the polymer clusters. It is reasonable to assume that the considerations described here are not exclusive to the PNIPAA–water system. They are also relevant to the hydrophobic interactions occurring in aqueous solutions of molecules with long hydrocarbon chains as well as to the sol–gel transition in physical gels.

It can be concluded that the fast response of PNIPAA observed at the VPT makes this polymer a good candidate for sensor applications involving light transmission. For uses in drug delivery systems, where solvent expulsion is required, the diffusion coefficient governing the release rate changes from about  $10^{-7}$  cm<sup>2</sup>/s below the VPT temperature to about  $10^{-17}$  cm<sup>2</sup>/s at temperatures above it.

## Conclusions

In pure water the cross-link ratio changes the swelling capacity of PNIPAA hydrogels but has no measurable

effect on the temperature of the phase transition. High-sensitivity isothermal microcalorimetry and DSC measurements at extremely low scanning rate yield heat effects for fully swollen gels that are roughly twice those reported in the literature. Under isothermal conditions the resulting system is practically in equilibrium, as shown by the value of the exothermal enthalpy which is independent of the size of the gel specimen in the temperature range 20–40 °C.

The swelling/deswelling process involves two stages with different time constants. The existence of the two stages is revealed by the appearance of a double peak at higher scanning rates and also by the hysteresis between heating and cooling cycles in DSC. Direct evidence of the two stages is furnished by SAXS observations. These show that following the prompt microphase separation, in which water-rich regions of the order of several thousand angstroms appear, extremely slow reorganization of the polymer-rich and solvent-rich interface occurs. The diffusion coefficient controlling this reorganization is of the order of  $10^{-17}$  cm<sup>2</sup>/s, which is typical of the glassy state.

**Acknowledgment.** This research was supported by the Széchenyi NRDP No. 3/043/2001 and the Hungarian National Research Fund (OTKA, Grant T 032211). We are grateful to Cyrille Rochas, Emese Fülöp, and György Bosznai for their invaluable assistance. Access to the small-angle beamline BM2 at the European Synchrotron Radiation Facility is gratefully acknowledged.

## References and Notes

- (1) Tanaka, T. *Phys. Rev. Lett.* **1978**, *40*, 820.
- (2) Shibayama, M.; Shirotani, Y.; Hirose, H.; Nomura, S. *Macromolecules* **1997**, *30*, 7307.
- (3) Kawasaki, H.; Sasaki, S.; Maeda, H. *Langmuir* **1998**, *14*, 773.
- (4) Tanaka, N.; Matsukawa, S.; Kurosu, H.; Ando, I. *Polymer* **1998**, *39*, 4703.
- (5) Geissler, E.; Hecht, A.-M. *J. Phys., Lett.* **1979**, *40*, L-173.
- (6) Tanaka, T.; Hocker, L. O.; Benedek, G. B. *J. Chem. Phys.* **1973**, *59*, 5151.
- (7) László, K.; Kosik, K.; Rochas, C.; Geissler, E. *Macromolecules* **2003**, *36*, 7771.
- (8) Horkay, F.; Zrínyi, M. *Macromolecules* **1982**, *15*, 1306.
- (9) de Gennes, P.-G. *Scaling Concepts in Polymer Physics*; Cornell University Press: Ithaca, NY, 1979.
- (10) Otake, K.; Inomata, H.; Konno, M.; Saito, S. *Macromolecules* **1990**, *23*, 283.
- (11) Shibayama, M.; Morimoto, M.; Nomura, S. *Macromolecules* **1994**, *27*, 5060.
- (12) Afroze, F.; Nies, E.; Berghmans, H. *J. Mol. Struct.* **2000**, *554*, 55.
- (13) Grinberg, N. V.; Dubovik, A. S.; Grinberg, V. Y.; Kuznetsov, D. V.; Makhaeva, E. E.; Grosberg, A. Y.; Tanaka, T. *Macromolecules* **1999**, *32*, 1471.
- (14) Li, S. K.; D'Emanuelli, A. *Int. J. Pharm.* **2003**, *267*, 27.
- (15) Salmerón Sánchez, M.; Hanyková, L.; Ilavský, M.; Monleón Pradas, M. *Polymer* **2004**, *45*, 4087.
- (16) Suetoh, Y.; Shibayama, M. *Polymer* **2000**, *41*, 505.
- (17) Shin, B. C.; Jhon, M. S.; Lee, H. B.; Yuk, S. H. *Eur. Polym. J.* **1998**, *34*, 1675.
- (18) Bale, H. D.; Schmidt, P. W. *Phys. Rev. Lett.* **1984**, *53*, 596.
- (19) Porod, G. In *Small-Angle X-ray Scattering*; Glatter, O., Kratky, O., Eds.; Academic Press: London, 1982.

MA048363X